

Ultrasensitive in vivo infrared spectroscopic imaging via oblique photothermal microscopy

Received: 29 October 2024

Accepted: 19 June 2025

Published online: 02 July 2025

Mingsheng Li^{1,2}, Sheng Xiao¹, Hongli Ni^{1,2}, Guangrui Ding^{1,2}, Yuhao Yuan^{1,2}, Carolyn Marar^{2,3}, Jerome Mertz^{2,3}✉, Ji-Xin Cheng^{1,2,3}✉

In vivo IR spectroscopy faces challenges due to poor sensitivity in reflection mode and low resolution at micrometer scale. To break this barrier, we report an oblique photothermal microscope (OPTM) to enable ultrasensitive IR spectroscopic imaging of live subjects at sub-micron resolution. Classic photothermal measurement captures only a small fraction of probe photons through an iris to extract the photothermal signal. Instead, OPTM uses a differential split detector placed on the sample surface to collect 500-fold more photons and suppress the laser noise by 12 fold via balanced detection. Leveraging its improved sensitivity, OPTM enables low-dose IR imaging of skin without photodamage. Depth-resolved in vivo OPTM imaging of metabolic markers beneath mouse and human skin is shown. Furthermore, we demonstrate in vivo OPTM tracking of topical drug contents within mouse and human skin. Collectively, OPTM presents a highly sensitive imaging platform for in vivo and in situ molecular analysis.

Label-free imaging of chemicals in live animals and human subjects is crucial for both basic research and clinical translation. Vibrational spectroscopic imaging has emerged as a highly sensitive, label-free platform to visualize molecular contents in living systems, advancing the study of biology and medicine¹. In particular, spatially offset Raman spectroscopy and coherent Raman scattering microscopy have been developed to image chemicals in the skin layers of live subjects^{2–4}. Compared to spontaneous Raman scattering, infrared (IR) absorption provides a cross section that is approximately eight orders of magnitude larger, and it is particularly sensitive to fingerprint vibrations⁵. Since William Coblentz introduced the IR spectrometer in the early 1900s to explore molecular structures⁶, IR spectroscopy has been significantly advanced. Among the various techniques, Fourier-transform infrared (FTIR) spectroscopy is extensively used in the fields of biological research, functional materials, and pharmaceuticals^{7,8}. The invention of the quantum cascade laser as a room-temperature semiconductor laser has facilitated highly sensitive IR spectroscopic imaging^{9,10}. Traditional IR spectroscopic imaging measures the loss of IR photons, which is not suitable for imaging live animals because IR

photons are attenuated and cannot penetrate through or reflect off an intact animal body. Photoacoustic IR microscopy circumvents the issue of low photon collection efficiency by using the weak-scattering photoacoustic wave as a readout of IR absorption^{11–13}. However, because IR photons attenuate in the acoustic coupling medium, photoacoustic IR microscopy cannot operate in an epi-mode, making it not applicable for universal in vivo imaging scenarios. FTIR and photoacoustic IR also face limitations in spatial resolution due to the diffraction limit of long IR wavelengths, making them inefficient for nanoscale chemical visualization in vivo. Using a near-field probe strategy to overcome the IR diffraction limit, atomic force microscope-infrared (AFM-IR) spectroscopy achieves 10-nm resolution^{14–16}. However, AFM-IR's limited penetration depth makes it unsuitable for volumetric imaging of biological samples.

Recently developed mid-infrared photothermal (MIP) microscopy addresses these limitations by using visible light to probe the mid-IR-induced thermal effects^{17–19}. Over the past few years, advances have been made towards wide-field measurement^{20–23}, video-rate imaging speed^{24,25}, micromolar-level sensitivity in fingerprint and silent

¹Department of Electrical and Computer Engineering, Boston University, Boston, MA, USA. ²Photonics Center, Boston University, Boston, MA, USA.³Department of Biomedical Engineering, Boston University, Boston, MA, USA. ✉e-mail: jmertz@bu.edu; jxcheng@bu.edu

windows^{17,26,27}, and 3D tomographic imaging capability^{28–30}. Despite these advances, *in vivo* MIP imaging has not yet been feasible due to limited sensitivity in visualizing chemical content in live animals. The epi-detection geometry is essential for *in vivo* imaging because photons cannot penetrate through the entire animal body due to strong scattering and absorption. In a classic epi-detected MIP microscope (Fig. 1a), the pump and probe beams are co-aligned and focused by a reflective objective onto a sample³¹. The scattered photons from the sample are collected by the same objective. An iris is employed before a remote photodetector to maximize the photothermal signals. However, the probe photons experience enormous scattering events in complex tissues, resulting in scattered photons losing their original propagation directions. Thus, using an objective and an iris to collect scattered photons is ineffective. While classic MIP can visualize chemical content in opaque samples, such as pharmaceutical tablets^{31,32} and thin tissue slices³³, it is not sensitive for *in vivo* measurement due to significant loss of highly scattered probe photons during back-propagation to the remote detector.

Here, we report an oblique photothermal microscope (OPTM) to enable high-sensitivity *in vivo* infrared spectroscopic imaging at sub-micron resolution (Fig. 1b). Instead of an iris before a remote detector, oblique photothermal detection is achieved by placing a differential split detector above the sample surface to collect epi-propagated probe photons with high efficiency. After multiple scattering within tissue, the forward-scattered photons from the focus are redirected to the backward direction before reaching the split detector. The propagation path of collected photons aligns obliquely from the focus to the split detector. The oblique optical detection or illumination using two fibers provides phase gradient information of samples for improved contrast, in which the phase gradient signal is proportional to refractive index variations (dn/dx , n is refractive index of sample, x is the lateral distance)^{34–37}. Yet, oblique detection itself only gives the phase gradient information, without molecular sensitivity.

In OPTM, the photothermal expansion of objects decreases their refractive index, thus reducing the deflection angle of the original probe path. Consequently, with the photothermal effect, one photodiode receives more photons while the other receives fewer. Thus, photothermal modulations from each half of the split detector have opposite signs. Subtracting the two signals of the split detector not only enhances the photothermal signal but also suppresses the laser noise via a balanced detection operation. In comparison, the classic photothermal microscopy only collects a small fraction of back-scattered photons from the focus³¹, which could be overwhelmed by the laser noise and detector noise. As shown below, our method increases the photon collection efficiency by 500 times and suppresses the laser noise by a factor of 12 via balanced detection. Leveraging its enhanced sensitivity, OPTM allows low-dose IR spectroscopic imaging of animal skin, thereby avoiding the risk of photodamage. Consequently, OPTM enables *in vivo* IR spectroscopic imaging of metabolic markers within animal and human skin. Moreover, OPTM allows for depth-resolved monitoring of topical drugs under mouse and human skin, unveiling the topical drug pathways and allowing quantitative evaluation of drug delivery efficiency. These advances highlight OPTM's potential in biomedical research and *in situ* molecular analysis.

Results

OPTM principle and simulation results

In an epi-detected MIP microscope³¹, IR and visible probe beams are combined via a dichroic mirror, focused by a reflective objective, then delivered onto a sample (Fig. 1a). The scattered probe photons are collected by the same objective. An iris is then placed before the remote photodetector to maximize the photothermal signals³⁸. In OPTM, both pump and probe beams are coaxially aligned. A split detector is positioned upon the sample surface, allowing it to collect

more epi-propagated probe photons (Fig. 1b). The photon propagation path aligns obliquely from the focus to the detector. The difference in intensity between the two halves of the split detector reveals the phase gradient information of an object within its surrounding medium, while the sum provides optical absorption information of the same object^{35,39}. Upon photothermal modulation, the intensity difference between both detectors yields photothermal phase gradient (PTPG) contrast. By taking the sum of the split detector signals, sum images are acquired simultaneously for comparison with PTPG images.

With the IR pump off, the object deflects the beam path due to different refractive indices between the object and its environment (Fig. 1c, top). The intensity difference between the split detector is proportional to the variation of refractive index in samples (dn/dx , n is refractive index of the sample, x is the lateral distance)^{34–37}. With the IR pump on, the object absorbs IR photon energy, undergoes thermal expansion, and creates a thermal lens in its surrounding environment (Fig. 1c, bottom). Because the thermal lens decreases the refractive index and increases the dimension of the object, it reduces the deflection angle of the original probe path. Compared to the IR-off status, one photodiode receives more photons while the other receives fewer photons. Consequently, the photothermal signals from each half of the split detector have opposite signs. Therefore, the subtraction operation enhances the photothermal signals. Meanwhile, equivalent to balanced detection, the subtraction operation suppresses the common-mode fluctuation, which is contributed by the probe laser noise^{40,41}.

To quantitatively demonstrate an improved photon collection efficiency, we conducted a Monte Carlo simulation to analyze the propagation of four million photons within a uniform scattering layer (Fig. 1d)^{42,43}. On the layer surface, the objective only collects the central photons within a finite angle of 30 degrees corresponding to the NA of the objective. In contrast, the split detector collects the scattered photons in a larger area as indicated with black dash box in Fig. 1d. We summed the photons on the detection areas of the split detector and the objective, divided it by the total photons on sample surface, and generated the photon collection efficiencies of the split detector and objective, as indicated by red and black curves in Fig. 1e. Although the slit within split detectors causes the leakage of photons, the collection efficiency of split detector can still reach to 39% while that of the objective is only ~0.1%. We computed the improvement factor by dividing the collection efficiency of the split detector by that of the objective. Our results indicate oblique detection offers around 500 times larger collection efficiency of scattered photons than the objective detection method (Fig. 1f). In summary, instead of filtering, OPTM uses a split detector to collect 500-fold more epi-propagated probe photons. Harnessing the inverse photothermal modulations on the split detector, OPTM employs the phase gradient signal as an efficient readout of photothermal contrast by subtracting the signals from the split detector.

OPTM instrumentation and signal processing

As illustrated in Fig. 2a, the OPTM combines a pulsed IR laser with a visible continuous wave laser as the pump and probe sources. The combined beams are delivered to the scan unit for beam scanning and focused by a reflective objective onto the sample. The scan unit includes a 2D galvo scanner for scanning laser beams, followed by reflective relay optics that include two concave mirrors (Fig. 2b). The use of reflective relay optics and a reflective objective mitigates the achromatic aberrations of the visible and IR beams^{24,44}. To enable oblique photothermal detection in the setup, a split detector consisting of two identical photodiodes is placed above sample surface (Fig. 2a). A slit between the detectors allows the laser beam to pass through. To facilitate oblique photothermal detection, we engineered a detection circuit on a customized PCB (Fig. 2c, d). Because oblique detection collects more probe photons, to avoid saturation, the split

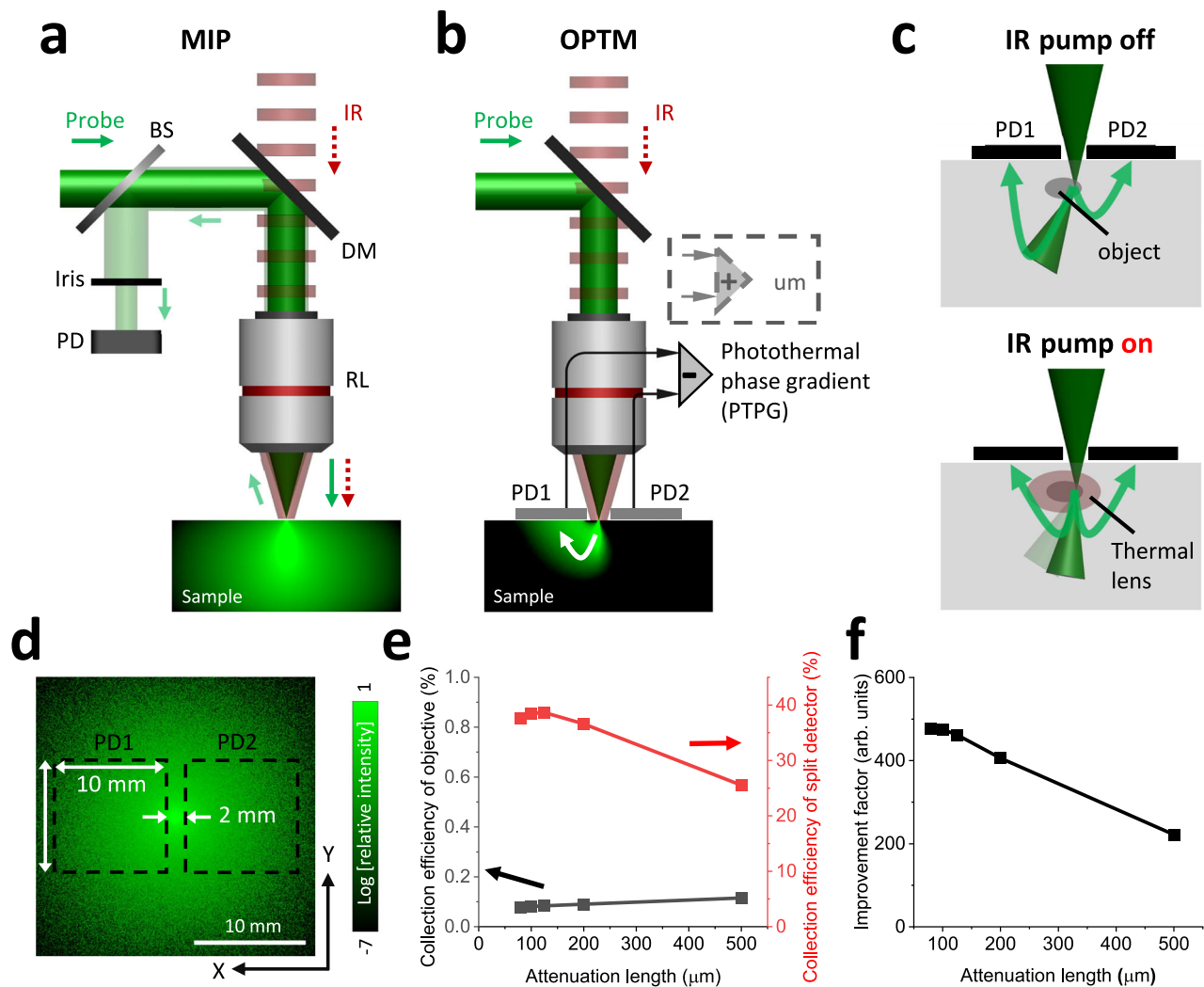


Fig. 1 | OPTM principle and simulation results. **a** Schematic of mid-infrared photothermal (MIP) microscope. **b** Schematic of oblique photothermal microscope (OPTM). Photons propagating to PD1 are shown in the sample box. **c** The principle of OPTM, illustrating the probe propagations at the status of IR on and off. **d** Monte Carlo simulation result of photon distribution on the surface of a uniform

scattering layer. **e** Photon collection efficiency of the split detector and objective. **f** The improvement factor in photon collection efficiency with oblique detection compared to the classic method. BS beam splitter, DM dichroic mirror, PD photodiode, RL reflective objective.

detector is biased by a 100-V DC source (V_B) to increase the saturation threshold of photodiodes. An RC low-pass filter is used to remove the high-frequency noise in the DC source. The signals from the two halves of the split detector are recorded independently, following the signal processing flowchart shown below. For comparison, an epi-detected MIP microscope is shown in Fig. S1, where a beam splitter is used to reflect the backward-propagated photons, then filtered by an iris before reaching a remote photodiode.

To generate photothermal phase gradient and sum images, we developed a signal processing flowchart as illustrated in Fig. 2e. Signals from each half of the split detector are split into AC and DC components. The DC components are recorded by a data acquisition card (DAQ). The sum of DC channels yields optical absorption information of the probe wavelength, while their difference provides the phase gradient of the objects. Each AC component is amplified and delivered to a lock-in amplifier for frequency-dependent demodulation of photothermal signals. The in-phase (X) and quadrature (Y) components are then output and recorded by a DAQ system. Through vector subtraction of AC components, OPTM images are generated to provide photothermal phase gradient (PTPG) information. The sum images are

generated by a vector summation operation for comparison with PTPG images.

OPTM imaging of microparticles in a scattering medium

To validate the principle of oblique photothermal detection, we employed the OPTM to image microparticles of well-defined sizes in a scattering medium. Specifically, 10- μ m PMMA beads were embedded in a scattering medium composed of 1:1 intralipid and PDMS mixture, then imaged using the OPTM (Fig. 3).

In the DC images, both halves of the split detector yield the phase gradient information of the microparticles (Fig. 3a). The DC signals show an inverted polarity at the two ends of the particles. The DC1 and DC2 images show the inverse phase gradients, akin to taking the first derivative of the refractive index from opposite horizontal directions. By subtracting and summing the DC1 and DC2 images, phase gradient DC and absorption DC images are generated (Fig. 3b). Figure 3c shows the plots of white lines in Fig. 3b to illustrate that the phase gradient measurement improves the contrast for visualizing particles in a scattering medium compared to absorption measurements. Because PMMA microparticles have negligible absorption at the probe

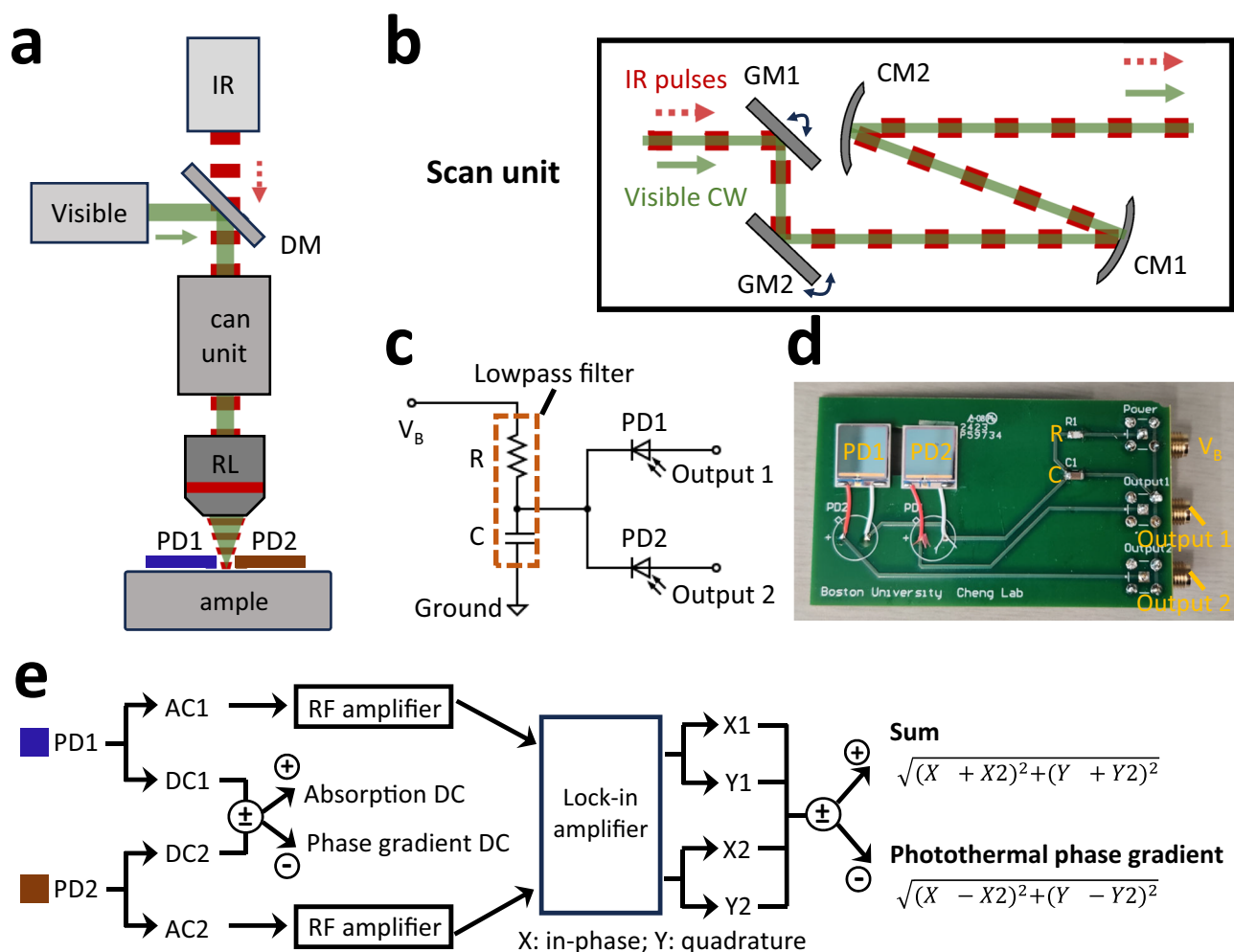


Fig. 2 | OPTM instrumentation and signal processing. **a** An oblique photothermal microscope (OPTM). **b** Details of scan unit. **c** Circuit diagram of split detector for collecting photocurrent from each photodiode independently. **d** Photo of split detector. **e** Signal processing flowchart of generating sum and photothermal phase

gradient images from split detector's signals. DM dichroic mirror, RL reflective objective, PD photodiode, CW continuous wave, GM galvo mirror, CM concave mirror.

wavelength of 532 nm, no visible features appear in the absorption DC images.

The photothermal images are acquired with the IR wavenumber of 1729 cm^{-1} , contributed by the stretching absorption of C=O bond in PMMA particles¹⁷. In the photothermal AC images, a lock-in amplifier demodulates frequency-dependent photothermal signals and generates both in-phase (X) and quadrature (Y) components of each split detector to form a complex photothermal response ($X+iY$) (Fig. 3d). The X and Y channels form a vector signal, where X is the real part and Y is the imaginary part. Figure 3e shows the vector signals of the split detector in 2D coordinates from the region of interest indicated by the black arrow in Fig. 3d. The vector signal of PD1 (X_1+iY_1) has an inverted direction compared to the vector signal of PD2 (X_2+iY_2). This indicates that the photothermal modulations of both photodiodes have opposite signs. Compared with the steady status of the IR pump off, with IR pump heating, one photodiode receives more photons while the other receives fewer. These results confirm the principle of oblique photothermal detection. Subsequently, through a post-processing step involving vector subtraction and summation, we derive photothermal phase gradient (PTPG) images and sum images (Fig. 3f). In our results, the signal-to-noise ratios (SNR) of PTPG and sum images reach 417 and 31, which indicates that OPTM is capable of imaging PMMA particles in a scattering medium with a 13-fold

improvement of SNR over sum image and sevenfold reduced laser noise. Additionally, we acquired the off-resonance images at 1770 cm^{-1} to demonstrate the bond-selectivity of OPTM imaging (Fig. S2). Figure 3g shows the spectra of PTPG and sum at the region of interest indicated with the white arrow in Fig. 3f. It indicates that OPTM enhances the spectroscopic intensity of particles in a scattering medium by over 10-fold in comparison with the sum measurement. Together, our results validate the principle of oblique photothermal detection, leveraging the differential response of split detectors to enhance photothermal signals while effectively suppressing laser intensity noise.

OPTM unveils two types of lipids in adipocytes under live mouse skin

Different lipid compositions are important indicators for skin cancer, such as sebaceous carcinoma⁴⁵. Coherent Raman scattering microscopy has allowed imaging of the total amount of lipids using C-H vibrational signals¹⁻³. Here, we demonstrate that OPTM can differentiate free fatty acid and lipid ester in individual adipocytes under live mouse skin. To compare the sensitivity of OPTM versus MIP microscope, we imaged adipocyte cells in the back skin of a live mouse using OPTM and MIP. Adipocytes on the epidermal layer of animal skin are vital to health as they form a barrier against external pathogens and